Available online at www.sciencedirect.com

SCIENCE DIRECT®

ELSEVIER

Palaeogeography, Palaeoclimatology, Palaeoecology 213 (2004) 231–250

PALAEO

www.elsevier.com/locate/palaeo

Possible Late Holocene equatorial palaeoclimate record based upon soils spanning the Medieval Warm Period and Little Ice Age, Loboi Plain, Kenya

Steven G. Driese[a,*], Gail M. Ashley[b], Zheng-Hua Li[a], Victoria C. Hover[c], R. Bernhart Owen[d]

[a]*Department of Earth and Planetary Sciences, University of Tennessee, Knoxville, TN 37996-1410, USA*
[b]*Department of Geological Sciences, Rutgers University, Piscataway, NJ 08854-8066, USA*
[c]*Department of Earth and Environmental Sciences, Rutgers University, Newark, NJ 07081-1819, USA*
[d]*Department of Geography, Hong Kong Baptist University, Hong Kong, People's Republic of China*

Received 25 April 2003; received in revised form 24 May 2004; accepted 2 July 2004

Abstract

Wetland and floodplain soils in the East African Rift of Kenya provide a record of changing palaeoclimate and palaeohydrology compatible with climate records for the mid-Holocene through the late Holocene Medieval Warm Period (~AD 800–1270) and Little Ice Age (~AD 1270–1850), documented previously in nearby lacustrine sites. Soils forming from volcaniclastic source materials in both Loboi Swamp and laterally adjacent Kesubo Marsh, two wetland systems of latest Holocene age, were investigated using micromorphology, whole-soil geochemical analysis, and stable isotope analysis of soil organic matter (SOM). Wetland formation was abrupt and possibly related to climate shift from drier conditions associated with the mid-Holocene and Medieval Warm Period, to wetter conditions associated with the Little Ice Age. Pre-wetland sediments are floodplain volcanic sandy silts comprising buried Inceptisols (SOM $\delta^{13}C = -15‰$ PDB) that fine upward to fine silt and clay, which are overlain by clays and organic-rich sediment (peat) (SOM $\delta^{13}C = -26‰$ PDB). Stable isotopes record an abrupt shift from 20 to 40% C3 vegetation (scrubland mixture of warm-season grasses and *Acacia*) to 100% C3 (wetland dominated by *Typha*) that occurred about 680±40 years BP (C-14 date from seeds). Soils developed on the periphery of the wetland show evidence for fluctuations in hydrologic budget, including siderite and redoximorphic features formed during wetter phases, and vertic (shrink–swell) and clay illuviation features developed during drier phases. Soils at Kesubo Marsh, located 2–3 km east of Loboi Swamp, consist of two buried mid-Holocene, 4000–4600 years BP (two C-14 dates from bulk SOM) Inceptisols developed from fluvially derived volcanic sand (SOM $\delta^{13}C = -15‰$ PDB) and separated from the latest Holocene surface soil (SOM $\delta^{13}C = -17.5‰$ PDB) by an unconformity and prominent stone line. Both the Loboi Swamp and Kesubo Marsh surface soils show increases in Zr, Fe, and S relative to buried soils, as well as higher leaching indices. Elevated Zr may reflect zircon

* Corresponding author. After June 15, 2004: Department of Geology, Baylor University, Waco, TX 76798-7354, United States. Tel.: +1 254 710 2361; fax: +1 254 710 2673.
E-mail address: Steven_Driese@baylor.edu (S.G. Driese).

doi:10.1016/j.palaeo.2004.07.009

grain inputs by either aeolian dust (during drier climate conditions) or fluvial sheetflood inputs, whereas higher leaching and elevated Fe and S represent pyritization associated with wetter conditions.

Keywords: Palaeoclimate; Wetland soils; Africa; Late Holocene; Stable carbon isotopes

1. Introduction

Wetlands are valuable potential repositories of information on climate and hydrology of Africa (Thompson and Hamilton, 1983). Development and expansion of wetlands are usually a function of both short- and long-term climate shifts and directly related to an increase in total precipitation (P) minus evapotranspiration (ET). However, springs and wetlands in tectonically active areas, like the East African Rift, may be related to the disruption of aquifers by faults and fractures (Le Turdu et al., 1999; Ashley et al., 2002; Deocampo, 2002) and so in such settings the growth of wetlands does not necessarily indicate a change to moister climate. Paleopedology, when combined with adequate geochronological controls, provides an excellent independent approach to interpret the geologic record of wetlands and allows a completely separate means to determine the paleoclimate within a geologically complex region. In this study, our objectives are: (1) to use soil morphology and micromorphology, bulk inorganic geochemistry, and stable isotopes of soil organic matter (SOM) to interpret the record of the abrupt shift from a floodplain environment dominated by C4 (Hatch-Slack) plants, to a wetland environment dominated by C3 (Calvin cycle) plants, about 700 years ago; (2) to show that formation of the wetland possibly coincided with a paleoclimate shift compatible with climate records for the drier Medieval Warm Period (~AD 800–1270) and the wetter Little Ice Age (~AD 1270–1850) documented previously in nearby lacustrine sites at Lakes Turkana and Naivasha (Mohammed et al., 1995; Verschuren et al., 2000; Verschuren, 2001; Lamb et al., 2003); and (3) to demonstrate that abrupt shifts in soil environments preserved in the geologic record, within active rift tectonic settings, can be interpreted as either direct evidence of palaeoclimate shifts that can supplement coeval lacustrine records, or as evidence for palaeotectonic processes in which springs abruptly develop due to fault processes.

1.1. Geological Setting

Loboi Swamp and Kesubo Marsh are located near the equator in the East African Rift Valley, within a broad alluvial area called the Loboi Plain, which is between Lake Baringo (fresh water) and Lake Bogoria (saline–alkaline) (Figs. 1 and 2). Loboi Swamp is about 3.5 km long and 0.5 km wide, and is fed by a series of warm (30–35 °C) freshwater springs that discharge into the south and west sides of the wetland (Fig. 2) (Ashley et al., 2002; Ashley et al., in press). Kesubo Marsh is 2–3 km east of the Loboi Swamp and lies at about the drainage divide between lakes Bogoria and Baringo (Fig. 2). The Loboi Plain is a locally swampy, subsiding alluvial fill of interbedded colluvial, fluvial, deltaic and lacustrine sediments that are Pleistocene to Holocene in age. Renaut and others have published extensively on the geology, hot springs and lake sediments in the environs of Lake Bogoria (Renaut, 1982, 1993; Renaut and Tiercelin, 1994; Renaut et al., 1986; 2000). However, the Holocene wetland soils were not examined in detail in these previous studies, nor did the previous studies employ micromorphological, whole-soil geochemical and stable carbon isotope studies in interpreting pedogenic processes. These additional research approaches permit greater resolution of interpretations of changes in pedogenic processes, sources of soil materials, and plant ecosystems that occurred in response to climate changes or tectonic processes.

1.2. Geomorphic setting

Loboi Swamp and Kesubo Marsh are located on the east side of the Loboi Plain against the lower "foothills" of the Laikipia Plateau (Tertiary volcanic fault blocks) (see Fig. 1.7 in Renaut, 1982). Loboi Swamp lies juxtaposed to trachyte flows, which are the primary aquifer units for the freshwater springs. Kesubo "Marsh" is actually a seasonally wet floodplain of the Sandai–Waseges River that flows north-

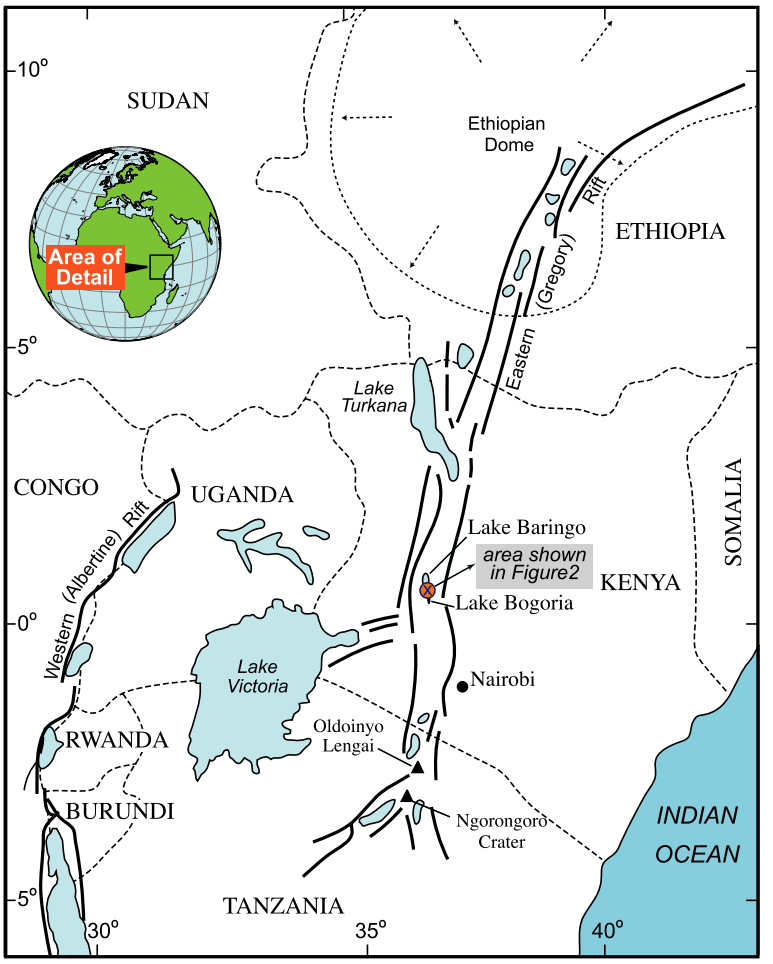

Fig. 1. Map showing locations of Loboi Plain, between Lakes Baringo and Bogoria in the Eastern Rift Valley of Kenya, modified after Ashley et al. (in press). (For colour see online version).

westward in a fault trough until it enters the rift valley, and then does a hairpin turn south and flows southeastward into Lake Bogoria at the Sandai delta (Fig. 2). The local drainage is unusual here because the Loboi River that lies to the west actually flows north into Lake Baringo, whereas the Sandai River flows to the south Fig. 2). Renaut (personal communication, 2001) attributes this to tilting fault blocks.

Kesubo Marsh is about 2 km wide at its maximum width and is framed by a small (1080 m high) volcanic upland to the west and the main volcanic upland (1240 m) (Waseges Range) on the east. *Acacia* and other C3 scrubland trees and shrubs occur along the seasonal Sandai River, whereas the western part of the floodplain is open C4 grassland. During the last El Niño (1997–1998) event a 2-m-deep channel was cut into the floodplain near the western margin of Kesubo Marsh. Heavy rains created a new drainage system by diverting some of the flow from the Sandai River to the west side of the swamp. The Kesubo soil profile described in this report was sampled from this natural exposure.

1.3. Climate setting and hydrology

The climate of the Loboi Plain is semi-arid, with precipitation of ~700 mm/year on the valley bottom and 1200 mm/year in the adjacent highlands; evapotranspiration is very high and is estimated to be ~2500 mm/year (Rowntree, 1989). Variation in precipitation occurs on a range of time scales, including semi-

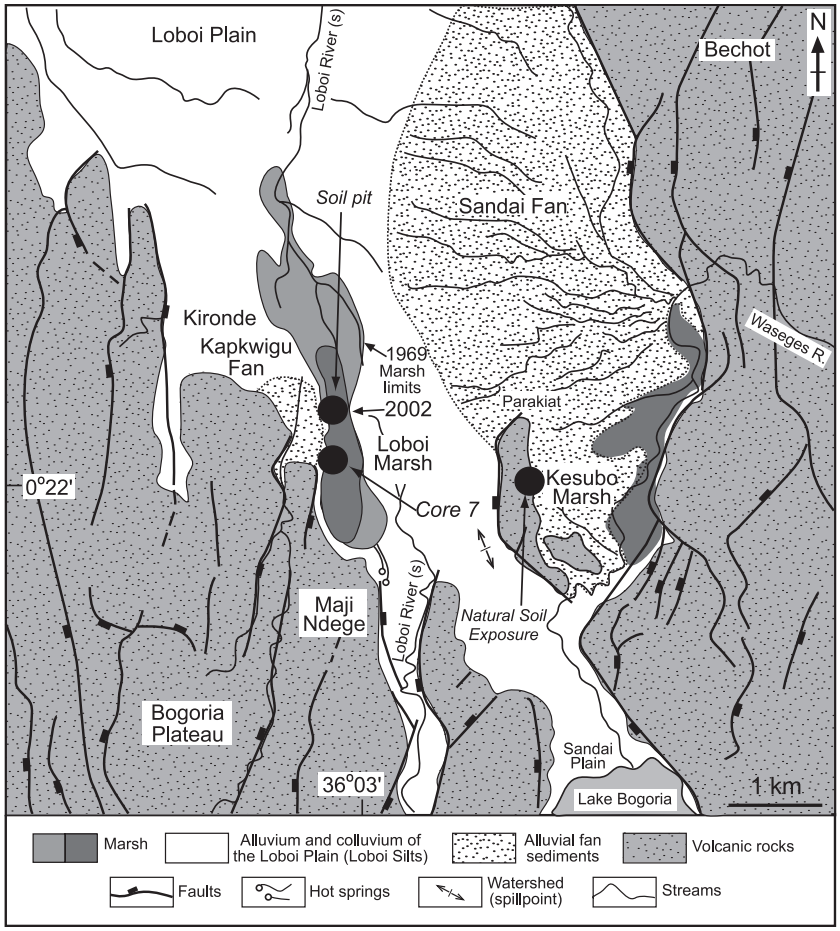

Fig. 2. Map showing locations of Loboi Swamp Soil Pit, sediment Core #7, and Kesubo Marsh soil sampling site, modified after Ashley et al. (in press). Note that soil study locations are about 3–4 km north of Lake Bogoria (shown in Fig. 1).

annual monsoonal rains in November and April, and El Niño and La Niña periods occur every 5–7 years (LaVigne and Ashley, 2001); longer-term variations in climate also occur, including circa 1500 year dry–wet climate cycles (e.g., Mohammed et al., 1995; Verschuren et al., 2000; Verschuren, 2001; Lamb et al., 2003) and orbitally forced precession (~20 ka), obliquity (~41 ka) and eccentricity (~100 ka) cycles (e.g., Pokras and Mix, 1985, 1987; Gasse et al., 1989; Ruddiman et al., 1989; DeMenocal and Bloemendal, 1995; Sirocko, 1996).

Water from springs discharging into Loboi Swamp is warm (35 °C), slightly acid to neutral (pH of 6.4–6.9), and has total dissolved solids of 250–350 mg/l (Ashley et al., in press). Water flowing in a small drainage through Kesubo Marsh, at the soil-sampling site, has a pH of 6.5, and Sandai River water, where it enters Lake Bogoria, has a pH of 7.4–7.8. A full suite of water data, including pH, electrical conductivity (EC), dissolved oxygen (DO), temperature, cations, anions, nitrates, Si, P, pCO_2, and O and C isotopes are reported elsewhere (Ashley et al., in press).

2. Materials and methods

2.1. Field sampling and laboratory analysis

In late June and early July of 2002, a 1 m (depth)×2 m (length) soil pit was hand-excavated at the northern

edge of Loboi Swamp in a dense stand of *Typha* (Fig. 2). Although the site at the time of excavation was dried and slightly desiccated, after 3 days seepage began to infiltrate the bottom of the pit. An additional 2 m high natural exposure of soil was sampled at Kesubo Marsh. The soil profiles at both sites were described and horizons defined using standard pedological techniques (Soil Survey Staff, 1998) and are reported in Appendix A. Bulk soil samples of about 200 g were collected at 5-cm intervals from 0 to 35 cm depth, and thereafter at 10-cm intervals to the base of the pit; charcoal was also sampled separately. Bulk soil samples were obtained from Kesubo Marsh at 10-cm intervals, beginning at 10 cm beneath the soil surface. Oriented thin-section samples were collected from each horizon at Loboi Swamp by driving a plastic electrical conduit box into the face of the soil pit; oriented soil clods were sampled from each horizon at Kesubo Marsh. Thin-section samples were also prepared from selected intervals of Loboi Swamp core #7, which penetrated to a depth of 4 m (Ashley et al., in press). All thin-section samples were later dried, epoxy-impregnated, and then commercially prepared. Micromorphological descriptions follow Brewer (1976), FitzPatrick (1993), and Stoops (2003).

After manual removal of macroscale organic matter and oven drying at 60 °C, pressed pellets were prepared from bulk, powdered soil samples and analyzed for selected major, minor and trace elements using a Philips wavelength-dispersive X-ray fluorescence (XRF) Analyzer (Singer and Janitzky, 1986). The XRF analytical protocol employed appropriate clay soil standards and reports major elements in oxide weight percent and trace elements in ppm (Appendices B and C, which are available directly from the first author, or can be accessed at http://www.baylor.edu/Geology). Whole-soil XRF chemical data were evaluated using a molecular-ratio approach, which does not require assumptions concerning soil parent materials (Retallack, 2001). Bulk organic carbon (OC) was determined by measuring loss-on-ignition (Kesubo Marsh) or by $\%CO_2$ yield after combustion for stable isotope analysis (Loboi Swamp), and bulk inorganic carbon (IC) was determined by weight loss after dissolution in HCl (Soil Survey Staff, 1995).

Dried soil (~60–200 mg sample to yield ~1 mg of carbon), after reaction with 1N HCl to remove carbonate, was loaded into a 25-cm-long quartz tube together with 500 mg of cupric oxide (CuO), 500 mg of purified granular copper (20–30 mesh) and a 2-cm-long platinum wire. Quartz tubes were sealed under vacuum, and samples combusted in a muffle furnace at 800 °C for 3 h, then allowed to cool to room temperature. The CO_2 gas evolved during combustion was collected and cryogenically purified, then analyzed by mass spectrometry (Finnigan Delta Plus). The results are expressed in $\delta^{13}C$ values with respect to the V-PDB standard.

$$\delta^{13}C = \left\{ \left[\left({}^{13}C/{}^{12}C\right)_{\text{sample}} / \left({}^{13}C/{}^{12}C\right)_{\text{PDB}} \right] - 1 \right\} \times 1000‰$$

Repeated combustion and analysis of USGS-24 graphite standard over the last 20 months during which these samples were analyzed gave a value of $-15.998 \pm 0.050‰$ (n=47) with a measurement standard deviation of 0.0141‰ (n=47), in good agreement with the value of $-15.99 \pm 0.10‰$ reported by Stichler (1995).

Chronology was provided by AMS radiocarbon dating of seeds from a core sample from 93- to 95-cm depth in Loboi Swamp core #1 (previously reported in Ashley et al., in press), and from two bulk SOM samples from 170 cm (4030±40 years BP, Beta-186020) and 180 cm (4450±40 years BP, Beta-186021) depth in the Kesubo Marsh soil profile.

3. Results

3.1. Soil morphological descriptions

3.1.1. Loboi Swamp

The Loboi Swamp surface soil (Appendix A) is a fine silty to fine loamy, mixed, isohyperthermic, shallow Typic Sulfaquept in USDA Soil Taxonomy (Soil Survey Staff, 1998). The substrate for the Loboi Swamp wetland consists of floodplain volcanic sandy silts and silty sands comprising Bw1b and Bw2b horizons of a buried Inceptisol (Aeric to Typic Tropaquept?), based on visual examination of the 1 m soil pit, as well as the 1.5–4 m long piston cores, (Figs. 3 and 4A); these 7.5 YR 3/1 (very dark gray) buried soils contain 1–3 mm diameter relict, partially decayed plant roots with 2.5 YR 4/6 (red) lepidochrocite (?) pore

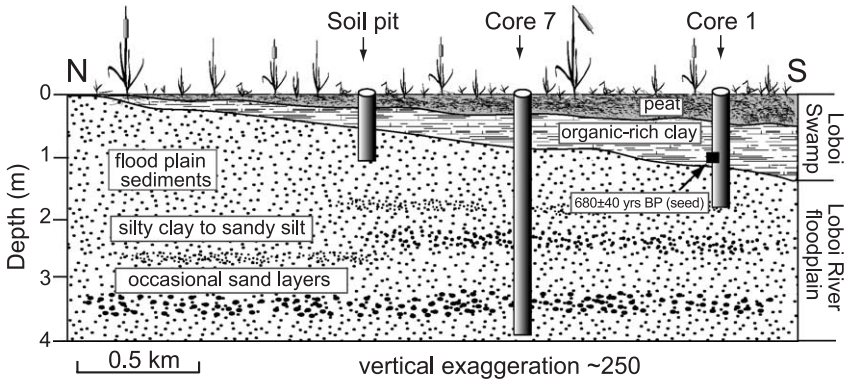

Fig. 3. North–south-oriented cross-section showing major soil and sediment lithologies encountered in cores in Loboi Swamp (see Fig. 2), modified after Ashley et al. (in press). Note that the soil pit was excavated at northern edge of Loboi Swamp, where fluctuations in hydrologic budget exert a stronger influence on pedogenesis.

linings, larger (1–5 cm) diameter, woody *Acacia* roots, and contain abundant very fine (sub-millimeter to millimeter diameter) siderite concretions.

The surface soil consists of both organic and mineral soil constituents. A peaty O horizon that ranges from 1 cm in the soil pit, to 1.5 m at the south end of Loboi Swamp occurs at the soil surface (Figs. 3 and 4). The underlying 7.5 YR 2.5/3 (very dark brown) A horizon consists of organic-rich silty clay that contains abundant spongy *Typha* roots up to 5 cm in diameter, and contains scattered "pockets" of charcoal; redoximorphic features (black Fe/Mn oxide and oxyhydroxide coatings) line root and insect macropores. The dark brown Bw1 (7.5 YR 3/3) and Bw2 (7.5 YR 3/2) horizons consist of silty clay with an overall higher clay content than the A horizon, but like the A horizon also contain abundant spongy *Typha* roots up to 5 cm in diameter, as well as redoximorphic features along soil macropores.

3.1.2. Kesubo Marsh

The surface soil profile at Kesubo Marsh is developed in volcanic-derived, fluvially deposited sand and fine gravel that has weathered to silty or sandy clay (Appendix A), and is classified as a coarse-loamy to sandy, mixed, isohyperthermic, shallow Aeric Tropaquept using USDA Soil Taxonomy (Soil Survey Staff, 1998) (Figs. 2 and 4B). Two buried mid-Holocene Inceptisols (Typic Tropaquepts?) occur beneath the surface soil, the boundaries of which are identified based on prominent textural discontinuities, including a prominent stone line that separates the

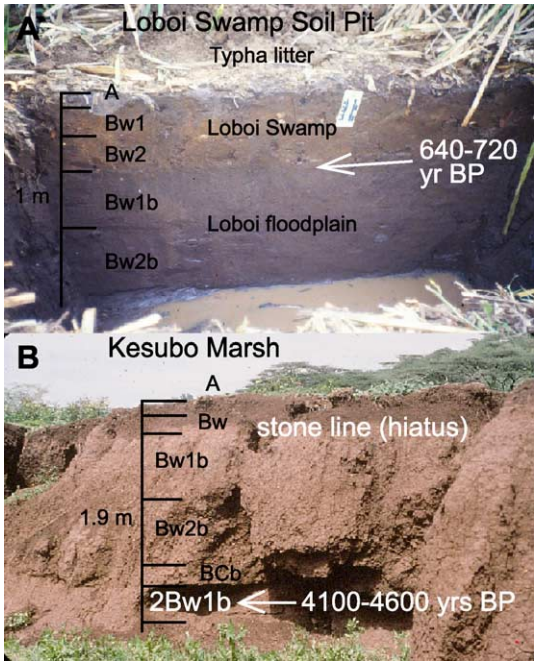

Fig. 4. Photographs of two field sites located on Fig. 2. (A) Soil pit, excavated in Loboi Swamp, showing sharp boundary between Bw horizons of buried, sandy silty to silty sand floodplain soil (Aeric or Typic Tropaquept?), and overlying late Holocene wetland clayey silt to silty clay soil (fine silty to fine loamy, mixed, isohyperthermic, shallow Typic Sulfaquept (Soil Survey Staff, 1998). (B) Natural soil exposure on western edge of Kesubo Marsh, showing two buried mid-Holocene clayey sand soils (Aeric or Typic Tropaquepts?), bounded by erosional surfaces and overlain by shallow surface soil (Coarse-loamy to sandy, mixed, isohyperthermic, shallow Aeric Tropaquept (Soil Survey Staff, 1998). (For colour see online version).

surface soil (0–35 cm) from the upper buried soil. The lower buried Inceptisol (2Bw1b horizon) ranges from dark grayish brown (10YR 4/2) to dark brown (10YR 3/3), has abundant 1–2 mm diameter root pores coated with black Mn oxides, medium subangular blocky peds, and contains abundant termite castings; an overlying (sharp, smooth boundary) B/Cb horizon at 140–160 cm depth exhibits relict horizontal bedding inherited from the parent material. The upper buried Inceptisol consists of Bw1b and Bw2b horizons that range from very dark brown (10YR 2.5/2) to dark brown (7.5 YR 3/2), and has a diffuse, upper fine to medium gravel band that defines a sharp, wavy boundary with the Bw horizon of the overlying modern soil. The morphology of the upper buried soil is very similar to that of the lower buried soil.

The surface soil commences with an A horizon consisting of dark brown (10YR 3/2) silty clay, with concentrated 1–3 mm diameter grass roots, fine to very fine granular peds, and abundant insect and termite castings. The underlying Bw horizon is brown (10YR 4/2) and mostly clay, with well developed, fine subangular blocky peds, and contains 10–15% yellowish red (5YR 5/8) limonite (?) or lepidochrocite (?) root and insect pore linings.

3.2. Soil micromorphology

3.2.1. Loboi Swamp

The A horizon (1–8 cm) consists of strongly bioturbated clay to silty clay, but also contains submillimeter thick depositional laminations. Important features include: (1) 5–10% yellow to orange, geopetally oriented illuviated clays with fine-scale microbanding that coat ped faces, root pores and fracture pores, (2) 10–20% black charcoal fragments concentrated into 2- to 5-mm-thick discrete layers, and (3) framboidal pyrite, much of which has been oxidized (Fig. 5A,B). A weak to moderately developed sepic–plasmic (bright clay) fabric is developed within the soil matrix. Other features include common medium to coarse roots (mainly *Typha* rhizomes), 0.5–2 mm diameter Fe/Mn oxide and oxyhydroxide glaebules, <1% angular to subrounded quartz and feldspar silt, diatoms (visible at high magnification and concentrated towards the soil surface; see Owen et al., in press), and insect egg cases (and/or seeds?), which are concentrated towards the soil surface.

The Bw1 (8–20 cm) and Bw2 horizons (20–30 cm) are composed of strongly bioturbated to weakly laminated clay that contains 10–15% yellow to orange, geopetally oriented illuviated clays with fine-scale microbanding and evidence for 3–4 distinct generations of clay infillings (oldest are red, intermediate are orange, and youngest are yellow), which coat ped faces, root pores and fracture pores (Fig. 5C,D). A moderate to strongly developed sepic–plasmic (bright clay) fabric (bimasepic to mainly masepic) is developed in the soil matrix. Other features include common fine to medium roots (mainly *Typha* rhizomes), 5–10% 0.1–2 mm diameter Fe/Mn oxide and oxyhydroxide glaebules, which are both embedded in the matrix and also occur as pore linings and hypocoatings, 5% disseminated 10–50 ìm diameter sphaerosiderite (?) crystals embedded in the matrix, ⩽1% angular to subrounded quartz and feldspar silt, and sparse diatoms visible at high magnification (Fig. 5E).

The Bw1b horizon (30–56 cm) is sandy silt, whereas the Bw2b horizon (56–100(+) cm) consists of silty, fine- to medium-grained sand (Fig. 5F,G). Silt is dominated by monocrystalline quartz and untwinned K-feldspar, whereas very fine- to medium-grained sand is composed of volcanic rock fragments that include both pumiceous/glassy and felted phenocrystic varieties, beta and embayed (volcanic) quartz, twinned plagioclase and K-feldspar, pyroxene and hornblende. Illuviation features include 1–3% yellow to orange, geopetally oriented illuviated clays with fine-scale microbanding and evidence for 3–4 distinct generations of clay infillings (oldest are red, intermediate are orange, and youngest are yellow) coating ped faces, root pores and fracture pores; common very fine to fine roots and sparse medium roots, including both *Typha* and another phytolith-bearing species; 5–10% Fe/Mn oxide and oxyhydroxide glaebules, 0.5–3 mm in diameter floating in soil matrix, and also occurring as replacements of ferromagnesian silicate grains; 1–2% papules (reworked illuviated clay coatings); 2% disseminated 5–10 ìm diameter sphaerosiderite (?) crystals floating in soil matrix (Fig. 5F–H).

3.2.2. Loboi Swamp core #7

Pelleted aggregates composed of organic-rich, silty clay to clayey silt dominate the upper 25 cm of Loboi Swamp core #7, and yellowish pedogenic clays coat the

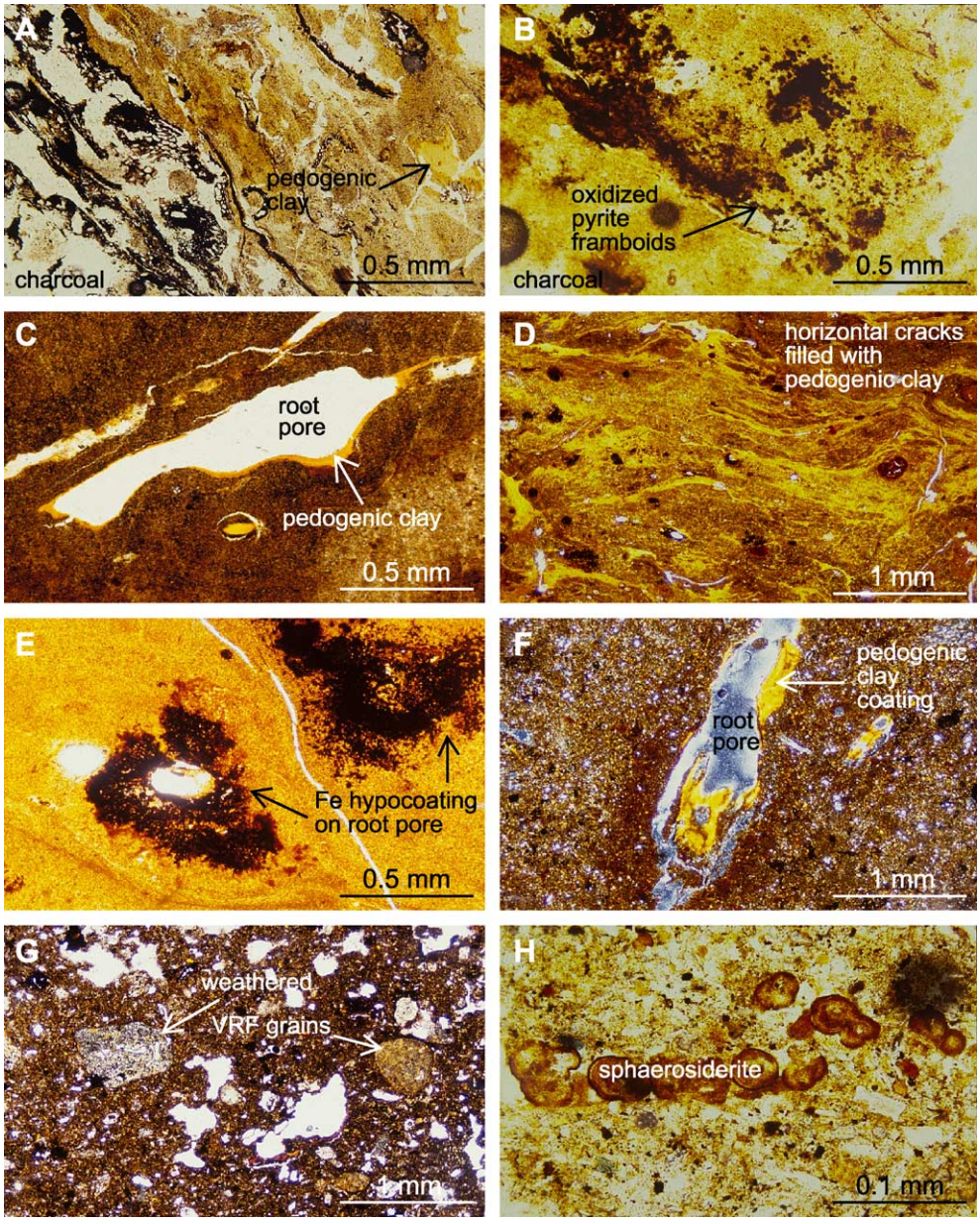

Fig. 5. Photomicrographs of wetland soil from Loboi Swamp Soil Pit (Fig. 4A), all taken in plane-polarized light (PPL), except for (F), which is in cross-polarized light (XPL). (A) A horizon, showing charcoal representing burned *Typha*. (B) A horizon, with pyrite framboids oxidized to FeO(OH). (C) Bw1 horizon, with root pores containing geopetal illuviated clay coatings. (D) Bw2 horizon containing horizontal to sub-horizontal cracks containing illuviated clay and geopetally oriented (vadose) silt infillings; note very fine root pores with dark-colored Fe–Mn oxide and siderite as coatings and hypocoatings. (E) Bw2 horizon, enlarged view of Fe–Mn oxide/oxyhydroxide and siderite coatings and hypocoating around root pores. (F) Bw1b Horizon, showing grass root pore lined by illuviated clay in sandy silt soil matrix. (G) Bw2b horizon, characterized by silty sand containing abundant weathered volcanic rock fragments. (H) Bw2b horizon showing abundant very fine sphaerosiderite crystals disseminated along soil macropore. For location of soil pit, see Fig. 2. (For colour see online version).

aggregate surfaces (Fig. 6A). Very finely crystalline siderite crystals are concentrated along macropores in association with decaying roots and other vegetation (Fig. 6B). Sand content increases progressively with depth to 125 cm, as does the abundance and size of siderite crystals coating macropore surfaces (Fig. 6C). Volcanic rock fragments are clearly identifiable within the sand fraction (Fig. 6D). The micromorphology of the core at greater depths is rather uniform and resembles that of the Bw1b and Bw2b horizons described previously from the Loboi Swamp soil pit.

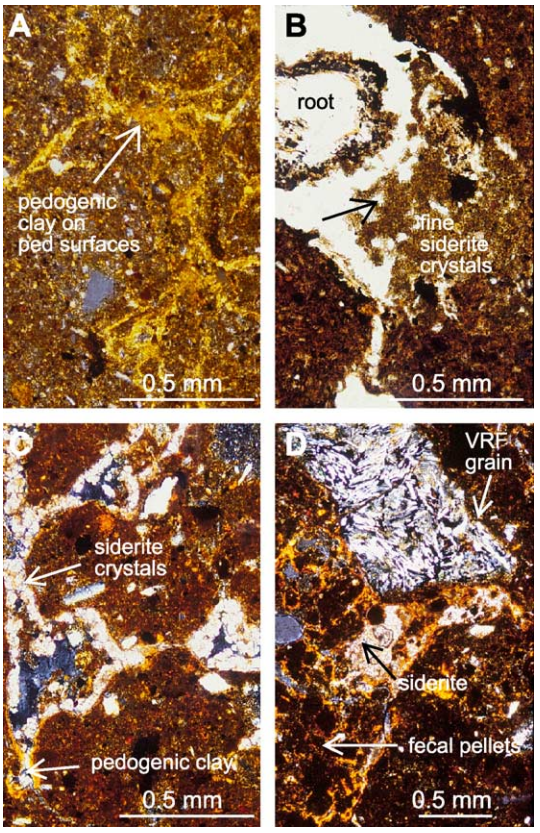

Fig. 6. Photomicrographs of buried floodplain soil from Loboi Swamp Core #7. All photographs are XPL except for (B). (A) Fine, pelletal aggregates (granular peds?) with clay argillans coating ped? surfaces (arrow), 23–25 cm depth. (B) Partially decayed root surrounded by very fine siderite crystals (arrow), 23–25 cm depth. (C) Pelletal aggregates with few pedogenic clay coatings and many coarser siderite crystal pore linings (arrows), 123–125 cm depth. (D) Weathered volcanic rock fragment (VRF) grains, very fine fecal pellets, and coarse siderite crystal pore linings (arrows), 123–125 cm depth. For location of Core #7, see Fig. 2. (For colour see online version).

3.2.3. Kesubo Marsh

The A horizon (0–10 cm) consists of dense fibric (undecayed organic) material, related to dense rooting by C4 grasses, and a silty clay soil matrix. Fe oxide or oxyhydroxide hypocoatings are commonly associated with root pores (Fig. 7A). The Bw horizon (10–34 cm) is silty clay in which the dark color is due to the abundance of amorphous Fe/Mn oxide or oxyhydroxide clay coatings of root and animal pores, as well as the abundance of finely disseminated organic matter (Fig. 7B). Pedogenic clay coatings of root macropores and of silt and sand grains are also locally well developed (Fig. 7C). The Bw horizons (34 cm to base of natural exposure at about 200 cm depth) of both buried Inceptisols, in contrast, are mostly clayey sand to silty sand, and have a generally similar micromorphology. Volcanic rock-fragment-rich, medium- to very coarse-grained sand, in which the grains are weathered to varying degrees, are the most abundant grain types (Fig. 7D,E). The volcanic rock fragments have both felted (flow-aligned) and non-felted (random or "jackstraw") plagioclase feldspar phenocrysts embedded in translucent to opaque matrices; both weathered and unweathered glass occurs within pyroclastic grains containing pumiceous textures. Volcanic-derived monocrystalline quartz grains with beta-type outlines, resorption rims and embayments are locally abundant, as are unweathered to partially weathered pyroxene and hornblende grains. Root pores are 0.2–2 mm in diameter, and are very similar to some of the sizes observed in the buried Bw horizons of the Loboi Marsh soil pit (Fig. 7F). Illuviated, birefringent clay coatings within root pores decrease in abundance downward, but are still present in the deepest horizon. The maximum amount of illuviated clay is estimated as 5%, which is similar to what was observed in the buried Bw horizons of the Loboi Marsh soil pit. Fe/Mn oxides and oxyhydroxides coat macropores in the Bw2b and B/Cb horizon (Fig. 7E). Termite castings are locally abundant and very deep within the soil profile. Minor amounts of zeolites occur in the deepest Kesubo horizon as an alteration product of some of the volcanic rock fragments. However, there are no pore-filling zeolites such as Renaut (1993) described in late Quaternary fluviolacustrine sediments in the Lake Bogoria Basin. Poorly preserved plant material with rare cell structure occurs in low concentrations in

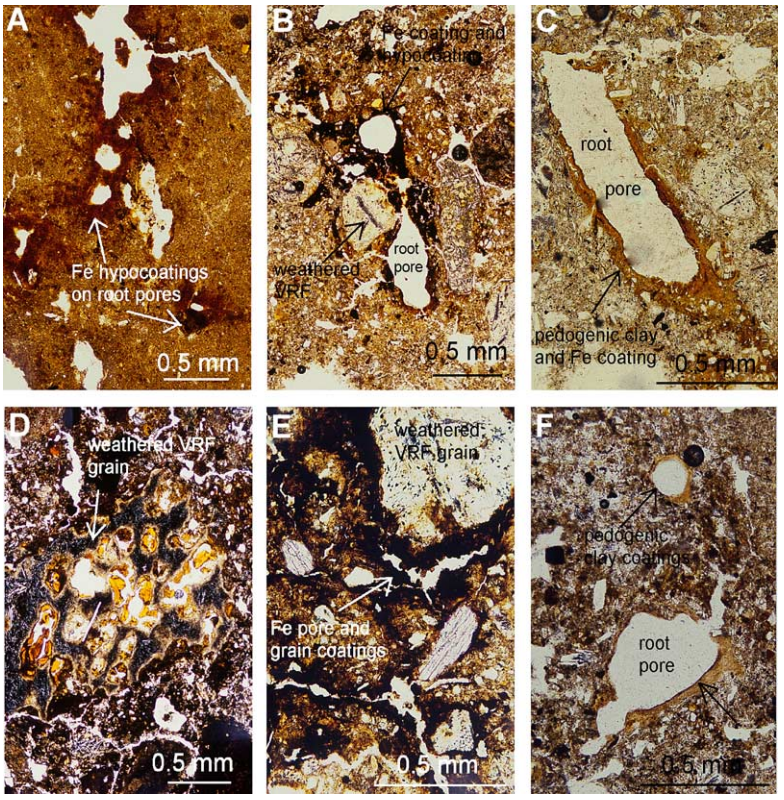

Fig. 7. Photomicrographs of surface and buried floodplain soils from Kesubo Marsh (Fig. 4B). All photographs are taken in PPL. (A) A horizon, clayey silt containing grass root pores with Fe oxide hypocoatings. (B) Bw horizon, showing root pores with Fe oxide coatings and hypocoatings, and weathered volcanic rock fragment (VRF) grains (arrows). (C) Bw horizon, with root pore and well-developed pedogenic clay coatings (arrow). (D) Bw1b horizon, volcanic glass preserved within vesicles of partially weathered VRF grain. (E) Bw2b horizon, showing Fe oxide pore and grain coatings and weathered VRF grains (arrows). (F) BCb horizon, with root? or insect? pores with pedogenic clay coatings (arrows). For location of Kesubo Marsh, see Fig. 2. (For colour see online version).

all horizons; some of the material appears burned, as would be expected in charcoal.

3.3. Stable carbon isotopes and geochronology

3.3.1. Loboi Swamp

The $\delta^{13}C$ values of soil organic matter (SOM) in the Bw horizons of the buried floodplain soils from the soil pit at the northern end of Loboi Swamp average between −14‰ to −15‰ PDB, as compared with average values of −24‰ to −26‰ PDB for the wetland soils comprising the upper 35 cm of the soil pit (Fig. 8A–C). The $\delta^{13}C$ values of SOM from core #7 from the southern portion of Loboi Swamp also range from −14‰ to −15‰ PDB, to a depth of 325 cm (Fig. 8B). A sharp inflection in the $\delta^{13}C$ curve occurs between the Bw1b and Bw2 horizons, where SOM values exhibit about a 10‰ shift within 20 cm of soil (Fig. 8B,C). Total organic C shows a similar dramatic shift from about 1 wt.% in the Bw1b and Bw2b horizons, to as high as 12 wt.% in the A Horizon (Fig. 8E).

3.3.2. Kesubo Marsh

The $\delta^{13}C$ values of soil organic matter (SOM) in the Bw horizons of the buried floodplain soils from the soil exposure at the western edge of Kesubo Marsh average about −15‰ PDB, as compared with average values of −17.5‰ PDB for the shallow surface soil comprising the upper 34 cm of the soil pit (Fig. 8A,B,D). A sharp inflection in the $\delta^{13}C$ curve occurs within the Bw1b and Bw horizons, where SOM values exhibit about a 2.5‰ shift within 20 cm of soil (Fig. 8D). Total organic C shows a similar

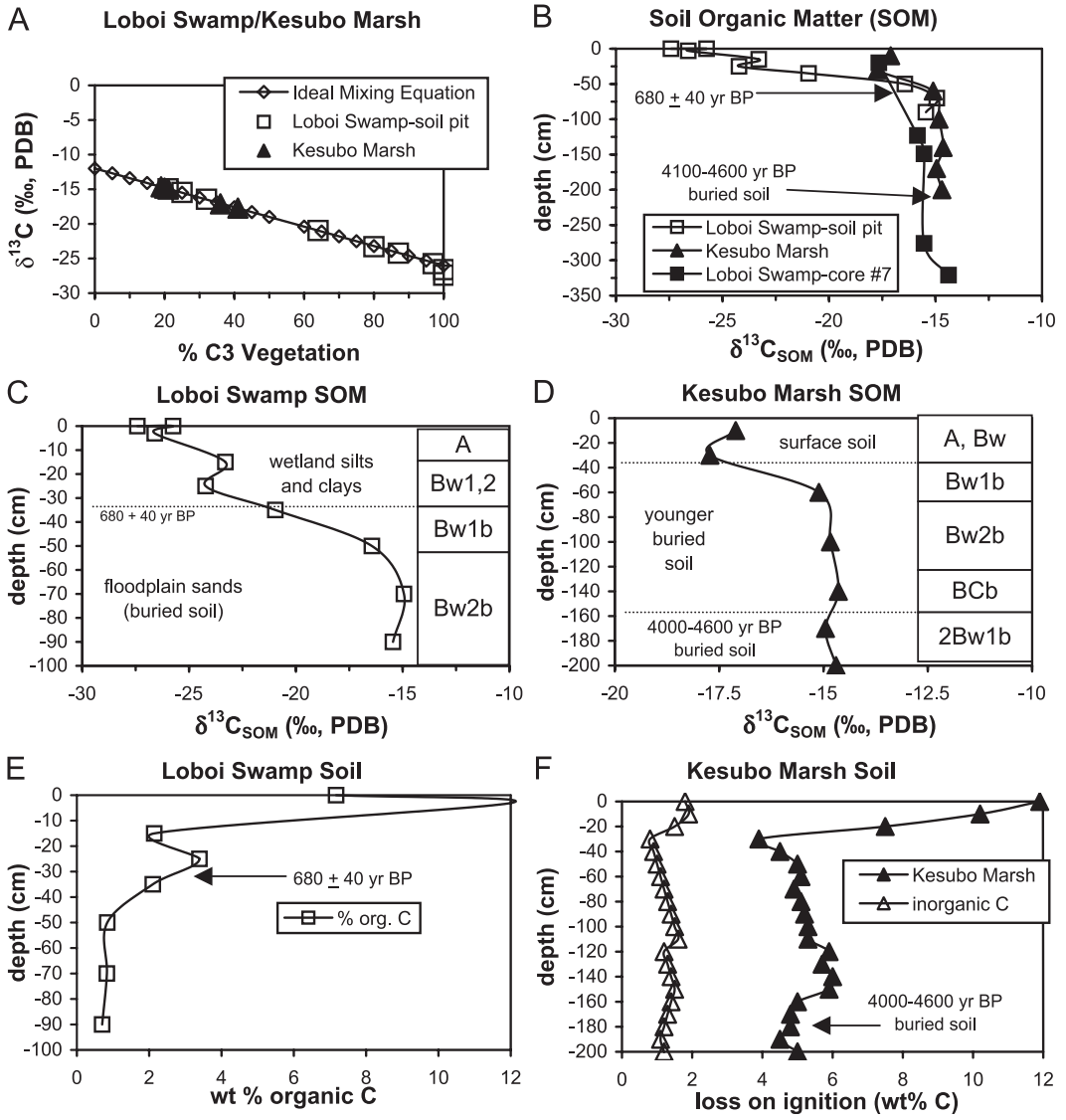

Fig. 8. Stable carbon isotope values of soil organic matter (SOM), and total carbon chemistry for Loboi Swamp and Kesubo Marsh soils. (A) Isotope mixing line calculated as $\delta^{13}C = -26(X) + -12(1-X)$, where X=fraction of vegetation that utilizes C3 photosynthetic pathway. The $\delta^{13}C$ values of soil organic matter are plotted on the mixing line in order to estimate % C3 vegetation contribution for samples from Loboi Swamp and Kesubo Marsh. More negative $\delta^{13}C$ values of SOM characterize C3-dominated ecosystems. (B) $\delta^{13}C$ values of SOM, versus depth, for all samples analyzed, showing total range from −14.5‰ to −26‰ PDB. (C) Details of Loboi Swamp depth profile for $\delta^{13}C$, which demonstrates a very abrupt −11.5‰ shift between more negative values characterizing the wetland soil, and less negative values typifying the subjacent floodplain soil. (D) Details of Kesubo Marsh depth profile for $\delta^{13}C$, which demonstrates an abrupt −2.5‰ shift between more negative values characterizing the surface soil, and the less negative values typifying the subjacent floodplain buried soils. (E) Total organic C measured as CO_2 yield on combustion for $\delta^{13}C$ measurement of Loboi Swamp SOM, showing very high organic C in surface wetland soil. (F) Total organic C measured as wt.% loss on ignition for Kesubo Marsh, showing very high organic C in surface soil.

dramatic shift from about 4 wt.% in the Bw1b and Bw2b horizons, to as high as 12 wt.% in the A Horizon (Fig. 8F).

3.3.3. C-14 chronology

A sample containing whole seeds obtained from the 93–95 cm depth interval in core #1 provided a

conventional radiocarbon age of 680±40 years using AMS dating (Ashley et al., in press). The wetland soil overlying the buried floodplain soils at Loboi Swamp is therefore no older than 640–720 years, and apparently formed after the end of the Medieval Warm Period (~AD 800–1270) and during the Little Ice Age (~AD 1270–1850) and post-Little Ice Age (1850 year to the present). Two samples of bulk SOM taken from the 170- and 180-cm depth intervals in the soil profile at Kesubo Marsh provided conventional radiocarbon ages of 4030±40 and 4450±40 years, respectively, also using AMS dating. The precursor floodplain system at Kesubo Marsh is therefore mid-Holocene in age, and is capped by a late Holocene surface soil that rests on an unconformity surface marked by a prominent stone line.

3.4. Inorganic (bulk) geochemistry

3.4.1. Loboi Swamp

The depth distributions of both Zr and TiO_2 show major inflections at the boundary between the wetland and the buried floodplain soils (Fig. 9A,B). Zr concentrations in the wetland soil increase by a factor of 3 as compared with the buried floodplain soil, indicating a significant increase in Zr input to the wetland during pedogenesis (Fig. 9B). The depth distribution of TiO_2 displays the reverse pattern in which TiO_2 decreases by about 20% in the wetland compared with the floodplain soil (Fig. 9A). The concentrations of both Fe_2O_3 and S exhibit a depth pattern of abrupt increase within the surface (wetland) soil that resembles the Zr depth pattern (Fig. 9A,B).

Molecular ratios related to leaching and hydrolysis, including the ratio of alumina to bases and Ba/Sr, are higher in the surface soil and decline in the buried floodplain soil (Fig. 9E). Molecular ratios related to calcification (ratio of alkaline earths to alumina) and salinization (ratio of alkalis to alumina) show weak surface (upper 10 cm) increase in calcification and increased salinization at the boundary between the surface soil and buried floodplain soil (Fig. 9F).

3.4.2. Kesubo Swamp

The A horizon represents an "outlier" with respect to its Zr and TiO_2 content; it contains twice the Zr content and 30% greater TiO_2 than the underlying Bw and Bw1b horizons (Fig. 9C,D). Overall, Zr has less percentage variation with depth, as compared with TiO_2. The concentrations of both Fe_2O_3 and S exhibit a depth pattern of abrupt decrease from the base of the surface soil, followed by a second maximum that corresponds to the base of the upper buried soil; this pattern more closely resembles the TiO_2 depth pattern (Fig. 9C,D).

Molecular ratios related to leaching and hydrolysis are both higher in the surface soil and towards the top of the upper buried soil, and decline with depth (Fig. 9G). The molecular ratio related to calcification declines progressively towards the soil surface, whereas the molecular ratio for salinization is highest at the boundary between the surface soil and upper buried soil, but then declines to the top of the lower buried soil, where there is a second maximum (Fig. 9H).

4. Interpretations and discussion

4.1. Soil ecosystem changes

There is clearly a sharp textural, mineralogical and geochemical discontinuity separating finer-grained,

Fig. 9. Depth plots of selected oxide-element chemistry and molecular ratios for Loboi Swamp and Kesubo Marsh soils. (A) Wt.% TiO_2 and $Fe_2O_3 \times 10^{-1}$ for Loboi Swamp, showing abrupt shift between wetland soil (lower TiO_2 and higher Fe_2O_3) and subjacent buried floodplain soil. (B) Concentrations (ppm) of Zr and S for Loboi Swamp, demonstrating abrupt shift between wetland soil (higher Zr and S) and subjacent buried floodplain soil. (C) Wt.% TiO_2 and $Fe_2O_3 \times 10^{-1}$ for Kesubo Marsh, illustrating abrupt shift between thin surface soil (higher TiO_2 and Fe_2O_3) and subjacent buried floodplain soils, but with a second maximum concentration corresponding to the base of the upper buried soil. (D) Concentrations (ppm) of Zr and S for Kesubo Marsh, showing abrupt shift between thin surface soil (higher Zr and S) and subjacent buried floodplain soils. (E) Molecular ratios for alumina/bases and Ba/Sr, for Loboi Swamp, demonstrating abrupt shift between more hydrolyzed wetland soil (higher base loss and Ba/Sr) and subjacent buried floodplain soil. (F) Molecular ratios for alkaline earths/alumina and alkalis/alumina, for Loboi Swamp, illustrating very weak surface calcification and strong salinization of wetland soil relative to subjacent buried floodplain soil. (G) Molecular ratios for alumina/bases and Ba/Sr, for Kesubo Marsh, showing abrupt shift between more hydrolyzed surface soil (higher base loss and Ba/Sr) and subjacent buried floodplain soils. (H) Molecular ratios for alkaline earths/alumina and alkalis/alumina, for Kesubo Marsh, demonstrating absence of calcification of surface soil and strong salinization of boundary between surface soil and top subjacent buried floodplain soil.

clayey-silty, more organic-rich wetland soil in the upper 35 cm of the Loboi Swamp, from sandy, less organic-rich sediments below (Figs. 4A, 5, 8B,C,E and 9A). The older, sandy, volcaniclastic-rich sediments, and the soils formed from them, represent a precursor floodplain system of the Loboi River, whereas the overlying finer, organic-rich clayey-silt sediments, and soils formed from them, are interpreted as "wetland " deposits that are less than 700 years old. The average $\delta^{13}C$ values of −14‰ to

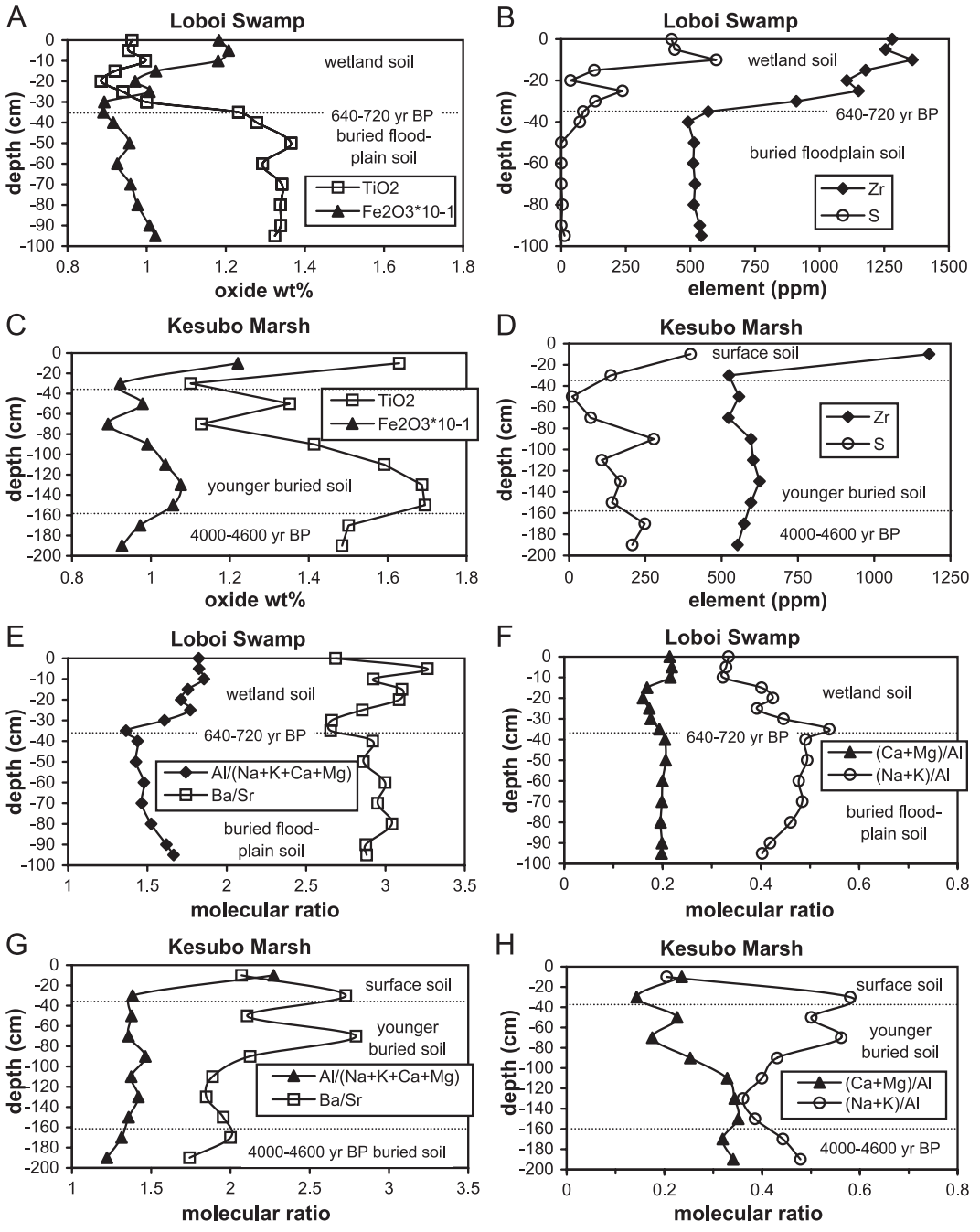

−15‰ PDB for soil organic matter (SOM) indicate that the precursor sandy floodplain was dominated by 20–30% C3 vegetation, and that it was likely a scrubland mixture of warm-season C4 grasses and C3 shrubs and trees such as *Acacia* (Fig. 8A). It is likely that an increase in mean annual precipitation associated with the end of the Medieval Warm Period and the beginning of the Little Ice Age about 700 years BP, and concomitant increase in spring discharge (Ashley et al., in press), rapidly converted the site to 100% C3 vegetation, consisting mainly of cattail (*Typha*) with average $\delta^{13}C$ values of −25‰ to −26‰ PDB for SOM (Table 1); the −11.5‰ shift in $\delta^{13}C$ values occurs over about 5–10 cm of soil thickness, suggesting a rapid onset of wetter climate and establishment of the wetland (Fig. 8C). An alternative hypothesis would be that fault rupture related to extensional rift tectonics created a pathway for groundwater to discharge across the floodplain surface, thereby creating the Loboi Swamp wetland system; unfortunately, the neotectonic history of this region is still poorly constrained in terms of geochronology, so testing this hypothesis against the soil record is not possible at this time (Le Turdu et al., 1999). Although *Cyperus papyrus* are present locally in the topographically lower parts of Loboi Marsh (Ashley et al., in press), they must not be significant contributors to the SOM in the areas sampled in the soil pit and cores; otherwise, the $\delta^{13}C$ values of SOM would have been heavier in the organic-rich wetland sediments, because this species of papyrus is a C4 plant with an average $\delta^{13}C$ value of −11.0‰ PDB (Aucour et al., 1993).

The surface soil at Kesubo Marsh records only a −2.5‰ shift in $\delta^{13}C$ values of SOM as compared to the two buried soils, which suggests a shift to a slightly greater C3 component (from 20% to 40% C3 vegetation; Fig. 8A,B,D). This change in carbon isotope values suggests either a climate shift or possibly tectonic tilting of the floodplain and resulting modifications to drainage at the site leading to wetter soil conditions; another possibility is that progressive displacement of C4 grasses by C3 shrubs and trees such as *Acacia* occurred in association with human disturbance at the site, which is currently grazed heavily by livestock maintained by the Tugen tribe. The Kesubo floodplain experienced episodic aggradation and erosion, as evidenced by the erosional boundaries between genetic soil bodies (Fig. 4B). In particular, the "stone line" occurring at the boundary between the Bw1b Horizon and the overlying Bw horizon suggests an episode of erosion and degradation on the mid-Holocene landscape prior to establishment of the late Holocene surface soil, and there may be a substantial hiatus of several thousand years separating the surface soil and buried soil (Appendix A).

4.2. Sources of soil materials

The surface soils at both sites consist of both wetland-produced materials (organic matter, diatoms; Owen et al., in press), as well as fine terrigenous material (detrital clay, quartz silt, zircon silt, etc.) that was either derived from flood events and trapped by the surface vegetation, or might also have been deposited as dust aerosols (possibly by "dust-devils"

Table 1
Summary of wetland and floodplain soils and inferred climate record, Loboi Swamp and Kesubo Marsh, Kenya

Depth (cm)	Loboi sediment	Loboi swamp soil pit	Kesubo marsh soils	Years before present (BP)	Lake Naivasha	Lake Turkana	Global Climate
0 to +2	*Typha* peat	(Oi horizon)	Fibric organic material	~150 BP–present	dry	?	Recent
0–35	Organic-rich clayey silt to silty clay	A, Bw1 and Bw2 horizons	A and Bw horizons	~150–700 BP	wet	wet	Little Ice Age
35–100(+) at Loboi; 35–200(+) at Kesubo	Silty sand to sandy silt; volcaniclastic sand-rich	Bw1b and Bw2b horizons	Bw1b, Bw2b, 2Bw1b horizons	(~700–1200 BP) to ca. 4500 BP	dry	dry	(Medieval Warm Period) to Mid-Holocene

Climate data for Lakes Naivasha and Turkana are from Mohammed et al. (1995), Verschuren et al. (2000), Verschuren (2001), and Lamb et al. (2003). Climate data for mid-Holocene in equatorial Africa from Talbot and Delibrias (1977), Gillespie et al. (1983), Blunier et al., 1995, and Barker et al., 2003. Chronology for Loboi Swamp from Ashley et al. (in press).

or other intense wind events). High concentrations of Zr at the soil surfaces at both sites might constitute evidence for a significant surface sheet flow or dust flux to the surface soils that includes zircon silt grains (Fig. 9B,D). This interpretation is also supported by micromorphological evidence indicating significant additions of illuviated clays to the surface soils within the last 600–700 years (Figs. 5A,C,D, 6A and 7C). Anthropogenic disturbance, related primarily to overgrazing by cattle and goats, as well as post-Little Ice Age warming and drying, has possibly accelerated the yield of locally derived dust due to loss of vegetative cover (Verschuren, 2001; Lamb et al., 2003; Ashley et al., in press). On a more global scale, Swezey (2001) recently documented significant increases in the eolian dust flux to sub-Saharan Africa during the past 3000 years, but whether these changes also affected the Loboi Plain region of Kenya is uncertain.

The buried soil that occurs beneath Loboi Swamp micromorphologically resembles the buried soils at Kesubo Marsh, but is not as coarse-grained (Figs. 5F,G, 6 and 7D–F). A dominant volcanic sand input is indicated for the buried soils at both sites. AMS dating of the top of the lower buried soil at Kesubo indicates that the Kesubo buried soils are possibly older (mid-Holocene) than the top of the buried soil in Loboi Swamp core #1 (late Holocene), but this does not preclude the possibility that the surface soil at Kesubo Marsh also contains a pedogenic record possibly correlative with a record of climate shift between the Medieval Warm Period and the Little Ice Age to post-Little Ice Age (Table 1).

4.3. Pedogenic processes

There is ample evidence for pedogenic processes sensitive to changing hydrology and water budget operating within the surface soil at Loboi Swamp, and to a lesser extent in the surface soil at Kesubo Marsh. During lower water input to Loboi Swamp, the wetland soil dried out, and soil processes were dominated by: (1) possible introduction of locally derived sheetflood fluvial sediment and/or dust aerosols to the soil (discussed previously), (2) soil desiccation and accompanying clay shrinkage/stress reorientation, (3) soil aeration, increased Eh and oxidation of organic matter (with probable fixation/precipitation of Fe/Mn oxides and oxyhydroxides), (4) occasional fire combustion of organic matter forming charcoal, and (5) illuviation of clays by percolating soil water containing clay colloid suspensions (Figs. 5 and 6). Wetting and clay swelling/stress reorientation, saturation and preservation of surface and subsurface organic matter, mobilization of Fe/Mn and precipitation of siderite in macropores due to lower redox conditions, are all processes that must correspond to times of higher water input to the swamp (Figs. 5 and 6).

Micromorphological evidence for fluctuating soil hydrology and attendant changes in pedogenic processes is not as pronounced in the Kesubo Marsh soils. Illuviated clay coatings of macropores provide evidence of clay translocation and free soil drainage, whereas Fe/Mn oxide pore-linings and matrix impregnations attest to episodes of soil saturation, lower Eh, and reduction of Fe, Mn, and other redox-sensitive elements (Fig. 7). Fluctuations in soil hydrology at both sites might correspond to decadal-scale climatic oscillations such as El Niño/La Niña, respectively, which have affected this region in the past 40–50 years (LaVigne and Ashley, 2001). Anthropogenic removal of water and diversion for irrigation of croplands could also account for post-1969 decreases in the size of Loboi Swamp (Ashley et al., in press) (Fig. 2). The climate record of nearby Lake Naivasha also indicates three significant periods of droughts during the Little Ice Age that ranged from 30 to 80 years in duration, which indicates that this region in East Africa is very susceptible to drought, even during generally wetter climate phases (Verschuren et al., 2000).

4.4. Inorganic Chemistry

Major differences exist in the redox chemistry, leaching and salinization at the two soil sites, which, in turn, are related to differences in soil hydrology. The surface soil at Loboi Swamp (Typic Sulfaquept) qualifies as a hydric soil (sensu Hurt et al., 1998) by virtue of being saturated and anaerobic in the upper 30 cm for some period during most years, whereas the Kesubo surface soil (Aeric Tropaquept), although apparently periodically wet, does not achieve the same degree of saturation and anaerobic conditions. Anaerobic conditions develop when oxidation–reduc-

tion reactions occur in the soil, which transfer electrons from donor to acceptor atoms; the major electron acceptors include O, N, Mn, Fe, S, and C, which are reduced in this order (Vepraskas and Faulkner, 2001). Sulfur transformations are biologically mediated, and like P and N transformations, are affected by the interaction between redox potential and pH.

The elevated concentrations of Fe and S, as well as the preservation of high concentrations of organic C, indicate that Fe and sulfate reduction are occurring in the surface soils at both sites (Figs. 8E,F and 9A–D). This is further supported by micromorphological evidence for framboidal pyrite precipitation at the soil surface at Loboi Swamp, as well as siderite precipitation in the deeper subsurface (Figs. 5B,H and 6). Maintenance of wetter conditions is also indicated the surface soils at both sites by molecular ratios indicating higher amounts of base loss and elevated Ba/Sr, as well as a general absence of surface calcification (Fig. 9E–H). The higher molecular ratio for salinization at the boundary between the surface soils and subjacent buried soils suggests a possible hydrogeologic control on distributions of Na and K caused by higher clay-silt content, lower-permeability soils overlying sandier, higher-permeability buried soils, or could simply be an effect of groundwater seepage (Fig. 9F,H).

5. Conclusions

Wetland soils developed in the semi-arid rift valley of Kenya record a hydrologic and water budget history that appears to complement late Holocene climate records obtained from Lakes Naivasha and Turkana by Mohammed et al. (1995), Verschuren et al. (2000), Verschuren (2001), and Lamb et al. (2003) (Table 1). The abrupt juxtaposition of finer-grained, clayey-silty, more organic-rich wetland soils with more negative (−26‰ PDB for Loboi Swamp; −17.5‰ PDB for Kesubo Marsh) $\delta^{13}C$ values of soil organic matter (wetland) on top of sandy, less organic-rich, buried Loboi floodplain soils with less negative (−14‰ to −15‰ PDB) $\delta^{13}C$ values is direct evidence for a dramatic shift from drier to wetter soil moisture conditions, which possibly corresponds with lacustrine climate records for the Medieval Warm Period (~AD 800–1270) and Little Ice Age (~AD 1270–1850). Alternatively, neotectonic processes of fault rupture may have abruptly created spring seeps, thereby resulting in formation of Loboi Swamp and Kesubo Marsh, but this cannot be tested without acquisition of a more detailed chronology for tectonism in this region (Le Turdu et al., 1999). In addition, the surfaces of the soils show evidence for increased ephemeral sheet flood or dust flux contributions of clays, quartz and zircon silt, perhaps reflecting increasing aridification since AD 1850, coupled with denudation of the landscape due to human disturbance. This study demonstrates that through detailed micromorphological, geochemical, and stable isotopic studies of wetland soils forming in semi-arid climates one can extract a hydrological and water budget record that, although not as high resolution as time-equivalent lacustrine records, can nevertheless provide possible palaeoclimate information that complements other proxy records.

Acknowledgments

Research was carried out under a permit (MOEST 13/00131C 103) from the Ministry of Education, Science and Technology of Kenya, A.G. Kaaria, senior assistant secretary. Research was supported by NSF EAR-0207705 to G.M Ashley and V.C. Hover. Acknowledgment is made to the donors of the Petroleum Research Fund, administered by the American Chemical Society, for partial support of this research (PRF 36498-AC8, Hover). We are grateful to Dr. Karega-Munene, Director of Archeology, National Museums of Kenya (NMK), for assistance with logistics. We are especially grateful to William Kimosop, Senior Warden for the Lake Bogoria National Reserve for his encouragement with the research. We appreciate the support of Maushe Kidundo and Musa Cheruiyot, Lake Bogoria Community Based Wetlands Project and the expertise of naturalist, Michael Kimeli. J. Bennett and W. Deane (Tennessee) kindly assisted with sample preparation and XRF analysis, respectively, and A. Ali (Kenya) and J. Cole (Stony Brook) assisted with field sampling.

Appendix A. Soil Descriptions

Loboi Swamp soil pit: N 00°22.455′; E 036°02.788′.

Surface soil: Fine silty to fine loamy, mixed, isohyperthermic, shallow Typic Sulfaquept (Soil Survey Staff, 1998).

Oi—1 cm to 0; peat comprised of moderately decomposed *Typha* blades, 5Y 2.5/1.

A—0–7.5 cm; very dark brown (7.5YR 2.5/3) clay loam; weak very fine granular structure; sticky, plastic; many very fine and fine roots, common coarse spongy *Typha* roots, with well-developed root mat at base; few pockets of charcoal and common partially decayed organic matter; many insect (ant?) burrows; black MnO stains on root pores; weakly calcareous; abrupt wavy boundary.

Bw1—7.5–20 cm; dark brown (7.5YR 3/3) clayey silt loam; moderate very fine subangular blocky structure; sticky and plastic; many very fine and fine roots, common coarse spongy *Typha* roots; common insect (ant?) burrows; slightly acid; clear wavy boundary.

Bw2—20–29.5 cm; dark brown (7.5YR 3/2) clayey silt loam; moderate very fine subangular blocky structure parting to weak granular structure; sticky and plastic; common very fine and fine roots, few coarse spongy *Typha* roots; noncalcareous; abrupt smooth boundary.

Buried soil: Aeric or Typic Tropaquept?

Bw1b—29.5–56 cm; very dark gray (7.5YR 3/1) sandy loam; moderate very fine to fine subangular blocky structure; firm; common very fine and fine roots; few very fine insect burrows; noncalcareous; clear smooth boundary.

Bw2b—56–100(+) cm; very dark gray (7.5YR 3/1) sandy loam; moderate very fine to fine subangular blocky structure; firm; few very fine and fine roots, few medium roots, including partially decayed *Acacia* woody root; few very fine insect burrows; 2% red (2.5YR 4/6) FeO(OH) root pore linings; noncalcareous; abrupt wavy boundary.

Kesubo Swamp (floodplain) soil exposure: N 00°22.019′; E 036°04.327′.

Surface soil: Coarse-loamy to sandy, mixed, isohyperthermic, shallow Aeric Tropaquept.

Oi—2 cm to 0; fibric layer comprised of slightly decomposed grass blades and leaf litter.

A—0–10 cm; dark brown (10YR 3/2) clayey silt loam; strong fine to very fine granular ped structure, parting to moderate medium granular; friable; many very fine, fine and medium roots; common termite castings and insect burrows; 1–5% rock fragments; noncalcareous; abrupt smooth boundary.

Bw—10–34 cm; dark grayish brown (10YR 4/2) to dark brown (10YR 3/2) silty clay loam; moderate fine subangular blocky ped structure; 10–15% yellowish-red (5YR 5/8) FeO(OH) pore linings and coatings on ped faces; common very fine and fine roots and few medium roots; common clay films on ped faces and in root pores; common termite castings and insect burrows; 5–10% rock fragments; noncalcareous; abrupt wavy boundary.

Buried soils: Aeric to Typic Tropaquepts(?).

Bw1b—34–67 cm; very dark brown (7.5 YR 2.5/2 to 10YR 2.5/2) fine sandy loam; moderate medium subangular blocky ped structure; firm; few very fine and fine roots; few faint clay films on ped faces and in root pores; 5% yellowish-red (5YR 5/8) FeO(OH) pore linings in upper 10 cm of horizon and 10–15% black MnO pore linings in lower 23 cm; 5–10% rock fragments, with prominent stone line containing 0.5–3 cm diameter basalt and trachyte pebbles at top of horizon; noncalcareous; clear wavy boundary.

Bw2b—67–142 cm; dark brown (7.5YR 3/2) coarse sandy loam; weak medium subangular blocky ped structure; firm; few very fine and fine roots, most stained with black MnO coatings; few termite castings; 10–25% rock fragments, up to 2–3 cm in diameter and dominated by basalt and trachyte; moderately acid; gradual wavy boundary.

BCb—142–159 cm; dark grayish brown (10YR 4/2) sandy loam; moderate fine to medium platy peds and relict bedding; firm; few very fine and fine roots, most stained with black MnO coatings; many termite castings; noncalcareous; abrupt smooth boundary.

2Bw1b—159–179 (+) cm; dark brown (10YR 3/3) sandy loam; moderate medium subangular blocky ped structure; firm; few very fine and fine roots, most stained with black MnO coatings; many termite castings; noncalcareous. (AMS C-14 dates of 4030±40 and 4450±40 years BP; Beta-186020 and 186021, respectively).

Appendix B. Bulk soil geochemistry of Loboi Swamp soil pit (all values are in wt.%)

Depth (cm)	Na_2O	MgO	Al_2O_3	SiO_2	P_2O_5	S	K_2O	CaO	TiO_2	V	Cr	MnO	Fe_2O_3	Co	Zn	Rb	Sr	Zr	Ba	Cu	Y	Hf	Total	Horizons	Bulk Density
0	1.44	0.55	16.91	47.59	0.133	0.0427	3.03	1.23	0.963	0.0009	0.0102	0.501	11.83	0.0027	0.0302	0.0187	0.0043	0.1281	0.0181	0.0027	0.0155	0.0025	84.45	O	n.d.
−5	1.36	0.62	16.61	47.04	0.164	0.0439	2.98	1.14	0.954	0.0007	0.0109	0.723	12.07	0.0035	0.0308	0.0187	0.0043	0.1255	0.0220	0.0021	0.0163	0.0023	83.94	A	1.01
−10	1.36	0.62	16.91	46.38	0.151	0.0600	2.98	1.15	0.997	0	0.0110	0.406	11.81	0.0032	0.0324	0.0195	0.0043	0.1359	0.0197	0.0025	0.0186	0.0027	83.07	Bwt1	1.08
−15	1.94	0.53	17.93	51.61	0.096	0.0128	3.70	0.92	0.920	0.0025	0.0099	0.290	10.23	0.0028	0.0279	0.0195	0.0037	0.1178	0.0180	0.0022	0.0133	0.0023	88.40	Bwt1	1.26
−20	2.12	0.50	18.01	52.35	0.094	0.0036	3.83	0.89	0.885	0.0005	0.0103	0.278	9.71	0.0026	0.0265	0.0188	0.0037	0.1105	0.0179	0.0022	0.0129	0.0022	88.88	Bwt1	1.16
−25	1.91	0.55	18.12	51.72	0.100	0.0237	3.66	0.96	0.940	0.0009	0.0106	0.298	10.07	0.0029	0.0274	0.0192	0.0038	0.1151	0.0170	0.0021	0.0132	0.0024	88.55	Bwt2	1.58
−30	2.26	0.55	17.60	53.50	0.105	0.0132	3.82	0.94	1.000	0.0006	0.0108	0.183	8.93	0.0029	0.0235	0.0168	0.0041	0.0910	0.0171	0.0023	0.0111	0.0021	89.08	Bwt2	1.20
−35	2.93	0.58	17.12	55.99	0.114	0.0085	4.08	1.02	1.232	0.0017	0.0119	0.272	8.91	0.0028	0.0167	0.0126	0.0056	0.0569	0.0233	0.0032	0.0075	0.0012	92.38	Bw1b	1.43
−40	2.69	0.68	17.38	53.95	0.127	0.0072	3.79	1.02	1.278	0.0030	0.0122	0.354	9.16	0.0027	0.0155	0.0113	0.0059	0.0491	0.0270	0.0034	0.0060	0.0009	90.56	Bw1b	1.50
−50	2.78	0.70	17.68	54.58	0.124	0	3.84	1.03	1.365	0.0017	0.0127	0.460	9.56	0.0035	0.0163	0.0112	0.0064	0.0514	0.0287	0.0033	0.0062	0.0011	92.26	Bw1b	1.50
−60	2.66	0.68	17.67	54.29	0.119	0	3.74	1.00	1.293	0.0019	0.0122	0.400	9.26	0.0034	0.0157	0.0110	0.0063	0.0511	0.0296	0.0035	0.0066	0.0011	91.25	Bw2b	1.35
−70	2.70	0.70	17.76	54.46	0.124	0	3.85	0.97	1.342	0.0022	0.0125	0.407	9.59	0.0031	0.0159	0.0113	0.0064	0.0518	0.0296	0.0035	0.0065	0.0011	92.04	Bw2b	1.26
−80	2.57	0.70	17.88	53.51	0.119	0.0004	3.70	0.95	1.338	0.0026	0.0117	0.350	9.77	0.0031	0.0157	0.0109	0.0064	0.0513	0.0305	0.0038	0.0065	0.0009	91.04	Bw2b	1.38
−90	2.35	0.77	18.45	52.60	0.120	0	3.57	0.95	1.339	0.0025	0.0121	0.390	10.07	0.0028	0.0165	0.0113	0.0063	0.0536	0.0284	0.0040	0.0068	0.0012	90.75	Bw2b	1.46
−95	2.25	0.78	18.62	52.32	0.119	0.0013	3.50	0.95	1.324	0.0027	0.0118	0.424	10.22	0.0029	0.0167	0.0113	0.0062	0.0542	0.0280	0.0041	0.0070	0.0010	90.65	Bw2b	1.39

Appendix C. Bulk soil geochemistry of Kesubo Marsh soil exposure (all values are in wt.%)

Depth (cm)	Na_2O	MgO	Al_2O_3	SiO_2	P_2O_5	S	K_2O	CaO	TiO_2	Cr	MnO	Fe_2O_3	Co	Ni	Zn	Pb	Rb	Sr	Zr	Ba	Cu	Total	Horizons	Bulk Density
−10	0.90	1.21	20.65	48.17	0.257	0.0398	2.54	0.99	1.630	0.0056	0.345	12.20	0.0016	0.0055	0.0235	0.0031	0.0143	0.0140	0.1180	0.0453	0.0068	89.17	A	1.47
−30	3.37	0.58	18.74	55.66	0.160	0.0137	4.92	0.67	1.101	0.0035	0.232	9.22	0.0015	0.0019	0.0151	0.0021	0.0116	0.0055	0.0524	0.0233	0.0017	94.79	Bw	1.58
−50	2.75	0.89	18.20	54.67	0.180	0.0010	4.24	1.03	1.352	0.0068	0.322	9.79	0.0024	0.0044	0.0162	0.0022	0.0122	0.0100	0.0557	0.0330	0.0033	93.56	Bw1b	1.57
−70	3.22	0.71	18.53	55.58	0.133	0.0071	4.72	0.79	1.128	0.0038	0.429	8.91	0.0017	0.0018	0.0159	0.0021	0.0121	0.0067	0.0523	0.0291	0.0040	94.30	Bw1b	1.57
−90	2.27	1.06	18.65	53.87	0.177	0.0278	3.98	1.11	1.414	0.0070	0.397	9.91	0.0014	0.0037	0.0175	0.0022	0.0127	0.0111	0.0596	0.0370	0.0073	93.02	Bw2b	1.64
−110	2.03	1.33	18.14	53.45	0.227	0.0107	3.62	1.43	1.591	0.0088	0.437	10.37	0.0017	0.0045	0.0185	0.0024	0.0125	0.0143	0.0604	0.0422	0.0100	92.80	Bw2b	1.61
−130	1.78	1.46	18.30	52.80	0.245	0.0169	3.39	1.43	1.687	0.0091	0.322	10.76	0.0016	0.0048	0.0181	0.0022	0.0123	0.0149	0.0625	0.0430	0.0120	92.36	Bw2b	1.59
−150	1.91	1.44	17.98	53.04	0.243	0.0141	3.50	1.48	1.695	0.0090	0.452	10.56	0.0016	0.0052	0.0179	0.0024	0.0121	0.0151	0.0596	0.0461	0.0117	92.48	BCb	1.70
−170	2.27	1.22	17.88	54.74	0.221	0.0248	3.85	1.44	1.501	0.0082	0.488	9.73	0.0014	0.0042	0.0175	0.0024	0.0123	0.0138	0.0574	0.0431	0.0083	93.532	Bw1b	1.78
−190	2.41	1.19	17.32	55.97	0.221	0.0207	3.99	1.60	1.485	0.0093	0.320	9.27	0.0014	0.0035	0.0165	0.0022	0.0125	0.0141	0.0552	0.0385	0.0076	93.942	Bw2b	1.78

References

Ashley, G.M., Goman, M., Hover, V.C., Owen, B.R., Renaut, R.W., Muasya, A.M., 2002. Artesian blister wetlands, a perennial water resource in the semi-arid rift valley of East Africa. Wetlands 22, 689–695.

Ashley, G.M., Maitima-Mworia, J., Muasya, A.M., Owen, R.B., Driese, S.G., Hover, V.C., Mathai, S., Goman, M.F., Renaut, R.W., Blatt, S.H., in press. Evolution of a freshwater wetland in a semi-arid environment, Loboi Marsh, Kenya, East Africa. Sedimentology.

Aucour, A.-M., Hillaire-Marcel, C., Bonnefille, R., 1993. A 30,000 year record of ^{13}C and ^{18}O changes in organic matter from an equatorial peatbog. Climate Change in Continental Isotopic Records, Geophysical Monograph, vol. 78, p. 351.

Barker, P., Williamson, D., Gasse, F., Gilbert, F., 2003. Climatic and volcanic forcing revealed in a 50,000-year diatom record from Lake Massoko, Tanzania. Quaternary Research 60, 368–376.

Blunier, T., Chappellaz, J., Schwander, J., Stauffer, B., Raynaud, D., 1995. Variations in atmospheric methane concentration during the Holocene epoch. Nature 374, 46–49.

Brewer, R., 1976. Fabric and Mineral Analysis of Soils, 2nd edition. Krieger Pub., New York. 482 pp.

deMenocal, P.B., Bloemendal, J., 1995. Plio–Pleistocene climatic variability in substropical Africa and the paleoenvironment of hominid evolution: a combined data-model approach. Paleoclimate and Evolution, with Emphasis on Human Origins. Yale University Press, New Haven, pp. 262–288.

Deocampo, D.M., 2002. Sedimentary processes and lithofacies in lake-margin groundwater-fed wetlands in East Africa. In: Ashley, G.M., Renaut, R.W. (Eds.), Sedimentation in Continental Rifts, vol. 73. Special Publication-SEPM, Tulsa, OK, pp. 295–308.

FitzPatrick, E.A., 1993. Soil Microscopy and Micromorphology. John Wiley and Sons, New York. 304 pp.

Gasse, F., Ledee, V., Massault, M., Fontes, J.C., 1989. Water level fluctuations of Lake Tanganyika in phase with oceanic changes during the last glaciation and deglaciation. Nature 342, 57–59.

Gillespie, R., Street-Perrott, F.A., Switsur, R., 1983. Post-glacial arid episodes in Ethiopia have implications for climate prediction. Nature 306, 680–683.

Hurt, G.W., Whited, P.M., Pringle, R.F. (Eds.), 1998. Field Indicators of Hydric Soils in the United States. US Department of Agriculture, Natural Resources Conservation Service. Version 4.0. 30 pp.

Lamb, H., Darbyshire, I., Verschuren, D., 2003. Vegetation response to rainfall variation and human impact in central Kenya during the past 1100 years. The Holocene 13, 285–292.

LaVigne, M., Ashley, G.M., 2001. Climatology and rainfall patterns: Lake Bogoria National Reserve (1976–2001) (unpublished report). Rutgers University, New Brunswick, NJ. 32 pp.

Le Turdu, C., Tiercelin, J.-J., Richert, J.P., Rolet, J., Xavier, J.-P., Renaut, R.W., Lezzar, K.E., Coussement, C., 1999. Influence of preexisting oblique discontinuities on the geometry and evolution of extensional fault patterns: evidence from the Kenya Rift using SPOT imagery. In: Morley, K. (Ed.), Geoscience of Rift Systems—Evolution of East Africa, Studies in Geology, vol. 44. American Association of Petroleum Geologists, Tulsa, OK, pp. 173–191.

Mohammed, M.U., Bonnefille, R., Johnson, T.C., 1995. Pollen and isotopic records in Late Holocene sediments from Lake Turkana, Kenya. Palaeogeography, Palaeoclimatology, Palaeoecology 119, 371–383.

Owen, R.B., Renaut, R.W., Hover, V.C., Ashley, G.M., Muasya, A.M., in press. Swamps, springs, and diatoms: wetlands regions of the semi-arid Bogoria–Baringo rift, Kenya: Hydrobiologia, 518, 59–78.

Pokras, E.M., Mix, A.C., 1985. Eolian evidence for spatial variability of Late Quaternary climates in tropical Africa. Quaternary Research 24, 137–149.

Pokras, E.M., Mix, A.C., 1987. Earth's precession cycle and Quaternary climatic change in tropical Africa. Nature 326, 486–487.

Renaut, R.W., 1982. Late Quaternary geology of the Lake Bogoria fault-trough, Kenya Rift Valley. Unpublished PhD dissertation, University of London. 498 pp.

Renaut, R.W., 1993. Zeolite diagenesis of late Quaternary fluvio-lacustrine sediments and associated calcrete formation in the Lake Bogoria Basin, Kenya Rift Valley. Sedimentology 40, 271–301.

Renaut, R.W., Tiercelin, J.J., 1994. Lake Bogoria, Kenya Rift Valley—A sedimentological overview. Tulsa, OK, Sedimentology of modern and ancient saline lakes. Special Publication-SEPM 50, 101–123.

Renaut, R.W., Tiercelin, J.J., Owen, R.B., 1986. Mineral precipitation and diagenesis in the sediments of the Lake Bogoria basin, Kenya Rift Valley. In: Frostick, L., et al., (Eds.), Sedimentation in the African Rifts, Special Publication-Geological Society, vol. 25, pp. 159–175.

Renaut, R.W., Tiercelin, J.J., Owen, R.B., 2000. Lake Baringo, Kenya Rift Valley, and its Pleistocene precursors. In: Gierlowski-Kordesch, E.H., Kelts, K.R. (Eds.), Lake Basins Through Space and Time, vol. 46. AAPG Studies in Geology, Tulsa, OK, pp. 561–568.

Retallack, G.J., 2001. Soils of the Past: An Introduction to Paleopedology, 2nd edition. Blackwell Science, Oxford. 416 pp.

Rowntree, K.M., 1989. Rainfall characteristics, rainfall reliability, and the definition of drought: Baringo District, Kenya. South African Geographical Journal 71, 74–80.

Ruddiman, W.F., Sarnthein, M., et al., 1989. Late Miocene to Pleistocene evolution of climate in Africa and the low-latitude Atlantic: Overview of Leg 108 results. In: Ruddiman, W., Sarnthein, M. (Eds.), Proceedings of Ocean Drilling Program, vol. 108, pp. 463–484.

Singer, M.J., Janitzky, P., 1986. Field and laboratory procedures used in a soil chronosequence study. U.S. Geological Survey Bulletin 1648. 49 pp.

Sirocko, F., 1996. The evolution of the monsoon climate over the Arabian Sea during the last 24,000 years. In: Heine, K. (Ed.), Paleoecology of Africa and Surrounding Islands. A.A. Balkema, Roterdam, pp. 53–69.

Soil Survey Staff, 1995. Soil Survey Laboratory Information Manual. Soil Survey Investigations. U.S. Government Printing Office, Washington, DC. Report 45, Version 1.0. 305 pp.

Soil Survey Staff, 1998. Keys to Soil Taxonomy, 8th edition. U.S. Government Printing Office, Washington, DC. 324 pp.

Stichler, W., 1995. Interlaboratory comparison of new materials for carbon and oxygen isotope ratio measurements. Reference and Intercomparison Materials for Stable Isotopes of Light Elements, IAEA TECDOC-825, pp. 67–74.

Stoops, G., 2003. Guidelines for Analysis and Description of Soil and Regolith Thin Sections. Soil Science Society of America, Madison, WI. 184 pp. + CD w/images.

Swezey, C., 2001. Eolian sediment responses to late Quaternary climate changes: temporal and spatial patterns in the Sahara. Palaeogeography, Palaeoclimatology, Palaeoecology 167, 119–155.

Talbot, M.R., Delibrias, G., 1977. Holocene variations in the level of Lake Bosumtwi, Ghana. Nature 268, 722–724.

Thompson, K., Hamilton, A.C., 1983. Peatlands and swamps of the African continent. In: Gore, A.J.P. (Ed.), Ecosystems of the World, Mires: Swamp, Bog, Fen and Moor, Regional Studies. Elsevier, Amsterdam, The Netherlands, pp. 331–373.

Vepraskas, M.J., Faulkner, S.P., 2001. Redox chemistry of hydric soils. In: Richardson, J.L., Vepraskas, M.J. (Eds.), Wetland Soils: Genesis, Hydrology, Landscapes and Classification. Lewis Publishers, New York, pp. 85–105.

Verschuren, D., 2001. Reconstructing fluctuations of a shallow East African lake during the past 1800 years from sediment stratigraphy in a submerged crater basin. Journal of Paleolimnology 25, 297–311.

Verschuren, D., Laird, K.R., Cumming, B.F., 2000. Rainfall and drought in equatorial east Africa during the past 1,100 years. Nature 403, 410–414.